Karttunen, Anssi; von Hertzen, Raimo; Reddy, JN; Romanoff, Jani

Bridging plate theories and elasticity solutions

Published in:
International Journal of Solids and Structures

DOI:
10.1016/j.ijsolstr.2016.09.037

Published: 01/01/2017

Document Version
Peer-reviewed accepted author manuscript, also known as Final accepted manuscript or Post-print

Please cite the original version:
Karttunen, A., von Hertzen, R., Reddy, JN., & Romanoff, J. (2017). Bridging plate theories and elasticity solutions. *International Journal of Solids and Structures*, *106-107*, 251–263.
https://doi.org/10.1016/j.ijsolstr.2016.09.037

Bridging plate theories and elasticity solutions

Anssi T. Karttunen[a,b,*], Raimo von Hertzen[a], J.N. Reddy[b], Jani Romanoff[a]

[a] *Aalto University, Department of Mechanical Engineering, FI-00076 Aalto, Finland*
[b] *Texas A&M University, Department of Mechanical Engineering, College Station, TX 77843-3123, USA*

Abstract

In this work, we present an exact 3D plate solution in the conventional form of 2D plate theories without invoking any of the assumptions inherent to 2D plate formulations. We start by formulating a rectangular plate problem by employing Saint Venant's principle so that edge effects do not appear in the plate. Then the exact general 3D elasticity solution to the formulated *interior* problem is examined. By expressing the solution in terms of mid-surface variables, exact 2D equations are obtained for the rectangular interior plate. It is found that the 2D presentation includes the Kirchhoff, Mindlin and Levinson plate theories and their general solutions as special cases. The key feature of the formulated interior plate problem is that the interior stresses of the plate act as surface tractions on the lateral plate edges and contribute to the total potential energy of the plate. We carry out a variational interior formulation of the Levinson plate theory and take into account, as a novel contribution, the virtual work due to the interior stresses along the plate edges. Remarkably, this way the resulting equilibrium equations become the same as in the case of a vectorial formulation. A gap in the conventional energy-based derivations of 2D engineering plate theories founded on interior kinematics is that the edge work due to the interior stresses is not properly accounted for. This leads to artificial edge effects through higher-order stress resultants. Finally, a variety of numerical examples are presented using the 3D elasticity solution.

Keywords: Interior plate, Saint Venant's principle, Clapeyron's theorem, elasticity solution, variational interior formulation, numerical examples

1. Background

1.1. Introduction

Engineering plate theories provide mathematically tractable descriptions for the bending and stretching of flat three-dimensional (3D) bodies by dealing only with two-dimensional (2D) variables defined on a reference surface, which is normally taken to be the mid-surface of the body at hand. In order to obtain 3D displacement, strain, and stress fields, the field variables are expanded through the plate thickness in an approximate sense. In the case of engineering plate theories based on assumed displacement fields, mid-surface deflections and rotations are the independent variables of choice, and integration through the plate thickness reduces the 3D theory to a *2D plate theory*.

Displacement-based 2D plate theories can be divided into two major classes: theories which consider transverse shear deformations and those that do not. The latter class relates to the study

Recompiled, unedited accepted manuscript. Cite as: *Int. J. Solids Struct* 2017;106–107:251–263 doi link

*Corresponding author. anssi.karttunen@iki.fi

of thin plates where the Kirchhoff plate theory is used rather exclusively (Szilard, 2004; Reddy, 2006). When it comes to shear-deformable plate theories, a number of options are available. The simplest and most well-known among them is the theory advanced by Mindlin (1951) which assumes the transverse shear deformation to be constant throughout the plate thickness and requires shear correction coefficients. Of particular interest to us are the so-called third-order plate theories which accommodate quadratic variations of the transverse shear strains and stresses with respect to the thickness coordinate (Reddy, 2006) and, thus, do not require shear correction coefficients.

The accuracy of 2D engineering plate theories may be tested by comparing their solutions with the exact 3D elasticity solutions available in the literature (Srinivas et al., 1969, 1970, 1973; Levinson, 1985; Piltner, 1988; Savoia and Reddy, 1992; Demasi, 2007; Batista, 2012). However, we find that such comparisons lack generality because they are mostly numerical and limited to certain cases. It is difficult to get detailed information on, for example, how well the analytical form of the utilized assumed displacement field matches its exact elasticity-based counterpart. To this end, we present in this paper an exact general 3D elasticity solution in the conventional form of 2D plate theories without using any kinematic, constitutive, or energetical assumptions. The elasticity solution takes the form of a third-order plate theory and introduces major improvements to the analytical treatment of similar 2D theories.

1.2. Third-order engineering plate theories

As already noted, third-order plate theories account for quadratic variation of the transverse shear strains and stresses through the plate thickness. This is accomplished by using an assumed displacement field which includes cubic powers of the thickness coordinate. Vlasov (1957) was possibly the first to develop a third-order plate theory. For surveys on third-order kinematics and plate theories, see the works of Jemielita (1990), Reddy (1990, 2003), and Reddy and Kim (2012). As pointed out by Reddy (1990), practically all third-order theories are in fact based essentially on the same displacement field.

The equilibrium equations for third-order plate theories in terms of stress resultants may be obtained by a vector approach where the 3D stress equilibrium equations are integrated with respect to the thickness coordinate (e.g., Levinson, 1980) (and they are the same as those used for the Mindlin theory), or by employing a variational method based on energy principles (e.g., Reddy, 1984). However, these two means are known to yield different governing equations. In more detail, variational (Lagrangian) methods lead to higher-order equilibrium equations than the Newtonian vector approach and, as a repercussion, Newtonian formulations are often labeled as "variationally inconsistent". To work towards sorting out this discrepancy, we ask: *For what part of a plate is an assumed third-order displacement field actually good for?* After all, the interior and boundary regions of a plate are two separate entities. For a detailed answer, we turn to 3D linear elasticity.

1.3. Exact elasticity solutions for plates

The most general state of stress within a linearly elastic, isotropic, homogeneous plate with stress-free upper and lower faces can be decomposed into three parts: (1) interior state, (2) shear state, and (3) Papkovich–Fadle state (Gregory, 1992; Wang and Zhao, 2003; Zhao et al., 2013). Detailed, general 3D elasticity solutions for plates which account for all three states have been given by Cheng (1979), Wang (1990, 1991), Piltner (1991, 1992a), and Batista (2015).

Piltner (1992a) constructed all displacement solutions that satisfy the stress-free boundary conditions on the upper and lower plate faces. The solution for the interior bending state is presented in terms of a biharmonic mid-surface function which is expanded through the plate by powers of the thickness coordinate z. However, terms above the third-order z^3, do not contribute to the solution, that is, transverse interior shear is quadratic. The solutions for the shear and Papkovich–Fadle states are expanded through the plate by trigonometric and hyperbolic functions of z, respectively. The flexural part of the shear state does not experience any transverse deflections and on the mid-surface all displacements are zero. Therefore, the shear solution does not play a direct role in the bending of plates. Instead, the shear state finds its place beside the interior solution in the pure torsion of plates (Cheng, 1979). The Papkovich–Fadle state on the other hand has been studied extensively in the context of 2D elasticity (Timoshenko and Goodier, 1970; Barber, 2010). It may be used to develop a boundary layer solution to complement the interior state. Such an edge effect solution is always (also in Piltner's plate study) connected to a complex eigenvalue problem from which the decay rates for the edge effects are determined. In fact, it has been proven that both the shear and Papkovich–Fadle states are predominantly related to edge effects (Gregory, 1992). Thus, we conclude these two states to be of secondary interest in the study of conventional interior plate bending. Hereafter, the focus will be on the interior state, also known as the "plate theory part" (Gregory, 1992). It will be shown that the 3D interior bending solution by Piltner (1992a) takes the form of a 2D third-order plate theory once expressed in terms of mid-surface variables instead of the biharmonic mid-surface function. Displacement considerations will be complemented by Wang's (1991) 3D interior membrane solution.

Finally, we return to our question on the nature and applicability of third-order kinematics (Section 1.2): It would be too far-reaching to use third-order kinematics to model the states other than the interior. For one thing, transverse shear strains and stresses are quadratic in the plate interior but not in the boundary layer. This interior notion is of great importance because if our plate consists solely of the interior state, *the interior stresses of the plate act as surface tractions on the lateral edges of the plate and, thus, they contribute significantly to the total potential energy of the plate*. Currently this contribution is not accounted for in any variational formulations of 2D engineering plate theories founded on interior kinematics. We will fill this gap to prevent the interpretation that the Newtonian treatment to be presented herein is "variationally inconsistent".

1.4. Recent interior studies and the present one

While the 3D plate solutions discussed above are usually obtained via displacement potentials, interior solutions for 2D plane beams can be found by using the Airy stress function. Recently, exact interior solutions, which excluded end effects by virtue of Saint Venant's principle, were developed for isotropic and anisotropic 2D interior plane beams and these solutions were reduced to exact 1D third-order beam equations (Karttunen and von Hertzen, 2016a,c). In addition, it was verified that the interior stresses acting as surface tractions on the lateral end surfaces of the interior beams need to be accounted for in all energy-based considerations. In light of the interior beam developments, the purpose of the present study is to generalize the beam results to plates.

The rest of this paper is organized as follows. In Section 2, an interior problem is formulated for a rectangular plate and the implications of the interior definition are discussed. In Section 3, the general 3D elasticity solution to the formulated problem is studied. Exact 2D bending equations for the interior plate are presented in terms of mid-surface variables formed from the 3D solution. Section 4 is devoted to the variational formulation of the Levinson plate theory, which is a special case of the 3D interior elasticity solution. As a novel contribution, the formulation properly accounts for the work due to the interior stresses on lateral plate edges. Calculation examples are presented in Section 5. These include polynomial-based solutions for simply-supported and clamped plates subjected to uniform pressure. Finally, concluding remarks are given in Section 6.

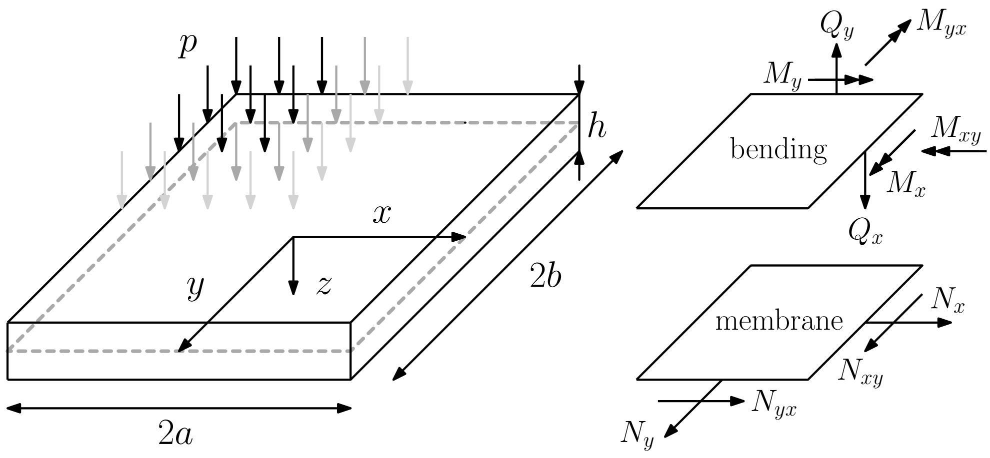

Figure 1: Rectangular interior plate subjected to a distributed load $p = p(x, y, -h/2)$ on the upper face. The plate may be divided into bending and membrane parts. The positive directions of the stress resultants are shown. The directions are reversed for opposite faces.

2. Interior problem formulation

2.1. Boundary conditions

A three-dimensional linearly elastic, isotropic, homogeneous plate under a distributed load p is shown in Fig. 1. The length, width and thickness of the plate are $2a$, $2b$ and h, respectively. The stress boundary conditions on the upper and lower faces of the plate read

$$\sigma_z(x, y, -h/2) = -p, \quad \sigma_z(x, y, h/2) = 0, \quad \tau_{xz}(x, y, \pm h/2) = \tau_{yz}(x, y, \pm h/2) = 0. \tag{1}$$

The boundary conditions are introduced in a *strong* (pointwise) sense for the upper and lower faces. On the lateral edges of the plate the tractions are specified through stress resultants as suggested by Fig. 1 and, thus, the boundary conditions on the lateral edges are imposed only in a *weak* sense (Barber, 2010). The stress resultants per unit length are calculated from the equations

$$\begin{Bmatrix} N_x \\ N_y \\ N_{xy} \end{Bmatrix} = \int_{-h/2}^{h/2} \begin{Bmatrix} \sigma_x \\ \sigma_y \\ \tau_{xy} \end{Bmatrix} dz, \quad \begin{Bmatrix} M_x \\ M_y \\ M_{xy} \end{Bmatrix} = \int_{-h/2}^{h/2} \begin{Bmatrix} \sigma_x \\ \sigma_y \\ \tau_{xy} \end{Bmatrix} z\, dz, \quad \begin{Bmatrix} Q_x \\ Q_y \end{Bmatrix} = \int_{-h/2}^{h/2} \begin{Bmatrix} \tau_{xz} \\ \tau_{yz} \end{Bmatrix} dz. \tag{2}$$

In view of the reciprocity of the shear stresses ($\tau_{xy} = \tau_{yx}$), we have $N_{xy} = N_{yx}$ and $M_{xy} = M_{yx}$. The replacement of the strong stress boundary conditions along the plate edges by the statically equivalent weak boundary conditions (stress resultants) implies that all detailed, exponentially decaying edge effects of the plate are eliminated by virtue of Saint Venant's principle and only the interior solution of the plate is under consideration. This means that an interior stress field is used to describe the whole plate domain. In fact, as will be discussed next, the interior solution represents practically a plate section which has been cut from a complete plate far enough from the real lateral boundaries at which true boundary conditions could be set. The general solution to the formulated interior plate problem for stress-free faces will be studied in Section 3. A uniform distributed load $p = p_0$ will be used as the particular contribution to elucidate some relevant features of the interior elasticity solution by Piltner (1992a) in more detail.

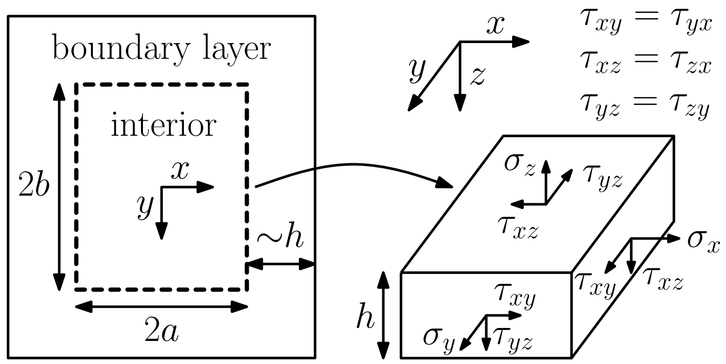

Figure 2: Rectangular plate consisting of an interior part and a boundary layer. When only the interior is studied, the interior stresses (positive directions shown) act as surface tractions and do work on the lateral edges of the plate.

2.2. Boundary layer and implications of the interior definition

Let us consider the rectangular plate with a boundary layer shown in Fig. 2. If pointwise boundary conditions were to be imposed on the outer edges of the boundary layer, the detailed distributions of the resulting stresses would bring about edge effects which decay exponentially towards the interior of the plate. That is to say, the edge effects are significant only in the boundary layer which, as a rule of thumb in isotropic cases, is as thick as the plate itself – the thinner the plate is, the weaker the edge effects are. Studying a plate which consists only of an interior part means that the boundary layer has been removed. This amounts to fully-developed interior stresses being active all-over the plate at hand, including the lateral plate edges, where they act as surface tractions as depicted on the right side in Fig. 2.

In terms of energetical considerations, the key feature of the interior plate definition is that the interior stresses acting as surface tractions on the lateral edges of the plate contribute to the total potential energy of the plate. In the case $p = 0$, the total potential energy of the interior plate in Fig. 1 can be written as (for all general interior solutions, in particular)

$$\Pi = U - W_s = U - W_s^{(+a)} - W_s^{(-a)} - W_s^{(+b)} - W_s^{(-b)}, \tag{3}$$

where the strain energy stored in the interior plate in terms of the stress and strain components is

$$U = \frac{1}{2}\int_V (\sigma_x \epsilon_x + \sigma_y \epsilon_y + \sigma_z \epsilon_z + \tau_{xy}\gamma_{xy} + \tau_{xz}\gamma_{xz} + \tau_{yz}\gamma_{yz})dV \tag{4}$$

and the work W_s due to the interior stresses on the lateral edges of the plate consists of

$$\begin{aligned} W_s^{(\pm a)} &= \pm \int_{-b}^{b}\int_{-h/2}^{h/2} \left[\sigma_x U_x + \tau_{xy} U_y + \tau_{xz} U_z\right](\pm a, y, z)\; dzdy, \\ W_s^{(\pm b)} &= \pm \int_{-a}^{a}\int_{-h/2}^{h/2} \left[\sigma_y U_y + \tau_{xy} U_x + \tau_{yz} U_z\right](x, \pm b, z)\; dzdy, \end{aligned} \tag{5}$$

where U_x, U_y and U_z are the 3D displacements in the directions of x, y and z, respectively. According to Clapeyron's theorem, the strain energy stored in an elastic body is equal to one-half of the work done by the surface tractions and body forces if they were to move (slowly) through their respective displacements from an unstressed state to the state of equilibrium (Sadd, 2014). In the present case, Clapeyron's theorem leads to $2U - W_s = 0$, which can be satisfied only trivially if the surface work W_s is not accounted for, as will be discussed further in Sections 4 and 5.

3. General 3D solution in the form of a 2D plate theory

3.1. Displacements, strains and stresses

Following Piltner (1992a) and Wang (1991), the general interior solution for a linearly elastic, isotropic, homogeneous plate with stress-free upper and lower faces can be written as

$$
\begin{aligned}
2G \cdot U_x = & -z\frac{\partial \Psi}{\partial x} - \frac{1}{4(1-\nu)}\left[h^2 z - 2(2-\nu)\frac{z^3}{3}\right]\nabla^2\frac{\partial \Psi}{\partial x} \\
& + (1+\nu)\frac{\partial H}{\partial x} - \frac{h^2}{24}\left[(3+4\nu) + 12\nu\left(\frac{z}{h}\right)^2\right]\nabla^2\frac{\partial H}{\partial x} - 2\nabla^2\Phi_x,
\end{aligned} \tag{6}
$$

$$
\begin{aligned}
2G \cdot U_y = & -z\frac{\partial \Psi}{\partial y} - \frac{1}{4(1-\nu)}\left[h^2 z - 2(2-\nu)\frac{z^3}{3}\right]\nabla^2\frac{\partial \Psi}{\partial y} \\
& + (1+\nu)\frac{\partial H}{\partial y} - \frac{h^2}{24}\left[(3+4\nu) + 12\nu\left(\frac{z}{h}\right)^2\right]\nabla^2\frac{\partial H}{\partial y} - 2\nabla^2\Phi_y,
\end{aligned} \tag{7}
$$

$$
2G \cdot U_z = \Psi + \frac{\nu z^2}{2(1-\nu)}\nabla^2\Psi + \nu z\nabla^2 H, \tag{8}
$$

where G and ν are the shear modulus and Poisson ratio, respectively. Function $\Psi(x, y)$ relates to bending and transverse shear (Piltner, 1992a), whereas $\Phi_x(x, y)$ and $\Phi_y(x, y)$ are stretching functions (Wang, 1991). Furthermore, we have

$$
\nabla^2 = \frac{\partial^2}{\partial x^2} + \frac{\partial^2}{\partial y^2}, \quad \nabla^4\Psi = \nabla^4\Phi_x = \nabla^4\Phi_y = 0, \quad H = \frac{\partial \Phi_x}{\partial x} + \frac{\partial \Phi_y}{\partial y}. \tag{9}
$$

Every term in the biharmonic functions Ψ, Φ_x and Φ_y can be multiplied by an arbitrary constant to be determined from boundary conditions. We note that Wang's membrane equations are written in such a form that they are consistent with Piltner's equations. In addition, we have made the correction $\alpha_C = 2-2\nu-2/\nu \to \alpha_C = -2/\nu$ to Wang's equations. The 3D displacements $U_x(x, y, z)$, $U_y(x, y, z)$ and $U_z(x, y, z)$ calculated from Eqs. (6)–(8) satisfy the Navier equations of elasticity.

As the first step towards presenting the above 3D displacement solution in the form of a 2D plate theory, we define the following three deflection and two rotation variables on the mid-surface

$$
\begin{Bmatrix} u_x(x,y) \\ u_y(x,y) \\ u_z(x,y) \\ \phi_x(x,y) \\ \phi_y(x,y) \end{Bmatrix} \equiv \begin{Bmatrix} U_x(x,y,0) \\ U_y(x,y,0) \\ U_z(x,y,0) \\ \frac{\partial U_x}{\partial z}(x,y,0) \\ \frac{\partial U_y}{\partial z}(x,y,0) \end{Bmatrix} = \frac{1}{2G}\begin{Bmatrix} \left[(1+\nu) - \frac{h^2}{24}(3+4\nu)\nabla^2\right]\frac{\partial H}{\partial x} - 2\nabla^2\Phi_x \\ \left[(1+\nu) - \frac{h^2}{24}(3+4\nu)\nabla^2\right]\frac{\partial H}{\partial y} - 2\nabla^2\Phi_y \\ \Psi \\ -\frac{\partial}{\partial x}\left[\Psi + \frac{h^2}{4(1-\nu)}\nabla^2\Psi\right] \\ -\frac{\partial}{\partial y}\left[\Psi + \frac{h^2}{4(1-\nu)}\nabla^2\Psi\right] \end{Bmatrix}, \tag{10}
$$

where the first two for the membrane solution were also given by Wang (1991). Furthermore, we find the following important relations

$$
\phi_x = -\frac{\partial u_z}{\partial x} - \frac{h^2}{4(1-\nu)}\frac{\partial}{\partial x}\nabla^2 u_z, \quad \phi_y = -\frac{\partial u_z}{\partial y} - \frac{h^2}{4(1-\nu)}\frac{\partial}{\partial y}\nabla^2 u_z \tag{11}
$$

$$
\frac{\partial \phi_x}{\partial y} = \frac{\partial \phi_y}{\partial x}, \quad \frac{\partial \phi_x}{\partial x} + \frac{\partial \phi_y}{\partial y} = -\nabla^2 u_z. \tag{12}
$$

By using the mid-surface variables, the 3D displacements given by Eqs. (6)–(8) can be written as

$$U_x = u_x + z\phi_x - \frac{4z^3}{3h^2}\left(\phi_x + \frac{\partial u_z}{\partial x}\right) + \frac{\nu z^2}{2(1-\nu)}\frac{\partial}{\partial x}\left[\frac{\partial u_x}{\partial x} + \frac{\partial u_y}{\partial y} + \frac{z}{3}\left(\frac{\partial \phi_x}{\partial x} + \frac{\partial \phi_y}{\partial y}\right)\right], \tag{13}$$

$$U_y = u_y + z\phi_y - \frac{4z^3}{3h^2}\left(\phi_y + \frac{\partial u_z}{\partial y}\right) + \frac{\nu z^2}{2(1-\nu)}\frac{\partial}{\partial y}\left[\frac{\partial u_x}{\partial x} + \frac{\partial u_y}{\partial y} + \frac{z}{3}\left(\frac{\partial \phi_x}{\partial x} + \frac{\partial \phi_y}{\partial y}\right)\right], \tag{14}$$

$$U_z = u_z - \frac{\nu z}{1-\nu}\left(\frac{\partial u_x}{\partial x} + \frac{\partial u_y}{\partial y}\right) - \frac{\nu z^2}{2(1-\nu)}\left(\frac{\partial \phi_x}{\partial x} + \frac{\partial \phi_y}{\partial y}\right). \tag{15}$$

Note that the above expressions are valid for any Ψ, Φ_x and Φ_y. By neglecting the higher-order membrane contributions in Eqs. (13) and (14) and then reducing the displacements to a plane ($x - z$ or $y - z$) and making the plane strain to plane stress conversion $\nu \to \nu/(1+\nu)$, the exact interior displacement field for a narrow beam is obtained. For reference, see (Karttunen and von Hertzen, 2016a,c).

The membrane part of solution (6)–(8) will not be discussed further in this section, as it plays a relatively minor role in the bending of isotropic interior plates, or flat shells, when only small transverse deflections are of interest. With that said, alternative expressions considering only the bending of the plate read

$$U_x = z\phi_x - \frac{z^3}{6}\left(\frac{2-\nu}{1-\nu}\right)\frac{\partial}{\partial x}\left(\frac{\partial \phi_x}{\partial x} + \frac{\partial \phi_y}{\partial y}\right), \tag{16}$$

$$U_y = z\phi_y - \frac{z^3}{6}\left(\frac{2-\nu}{1-\nu}\right)\frac{\partial}{\partial y}\left(\frac{\partial \phi_x}{\partial x} + \frac{\partial \phi_y}{\partial y}\right), \tag{17}$$

$$U_z = u_z + \frac{\nu z^2}{2(1-\nu)}\nabla^2 u_z. \tag{18}$$

By introducing

$$\lambda = \frac{\nu E}{(1+\nu)(1-2\nu)} \quad \text{and} \quad e = \epsilon_x + \epsilon_y + \epsilon_z \tag{19}$$

the strains and stresses of the plate, with the exclusion of the membrane part, can be written as

$$\begin{aligned}
\epsilon_x &= \frac{\partial U_x}{\partial x} = z\frac{\partial \phi_x}{\partial x} - \frac{z^3}{6}\left(\frac{2-\nu}{1-\nu}\right)\frac{\partial^2}{\partial x^2}\left(\frac{\partial \phi_x}{\partial x} + \frac{\partial \phi_y}{\partial y}\right), && \sigma_x = \lambda e + 2G\epsilon_x, \\
\epsilon_y &= \frac{\partial U_y}{\partial y} = z\frac{\partial \phi_y}{\partial y} - \frac{z^3}{6}\left(\frac{2-\nu}{1-\nu}\right)\frac{\partial^2}{\partial y^2}\left(\frac{\partial \phi_x}{\partial x} + \frac{\partial \phi_y}{\partial y}\right), && \sigma_y = \lambda e + 2G\epsilon_y, \\
\epsilon_z &= \frac{\partial U_z}{\partial z} = -\frac{\nu z}{1-\nu}\left(\frac{\partial \phi_x}{\partial x} + \frac{\partial \phi_y}{\partial y}\right), && \sigma_z = \lambda e + 2G\epsilon_z, \\
\gamma_{xy} &= \frac{\partial U_x}{\partial y} + \frac{\partial U_y}{\partial x} = z\left(\frac{\partial \phi_x}{\partial y} + \frac{\partial \phi_y}{\partial x}\right) \\
&\quad - \frac{z^3}{3}\left(\frac{2-\nu}{1-\nu}\right)\frac{\partial^2}{\partial x \partial y}\left(\frac{\partial \phi_x}{\partial x} + \frac{\partial \phi_y}{\partial y}\right), && \tau_{xy} = G\gamma_{xy}, \\
\gamma_{xz} &= \frac{\partial U_x}{\partial z} + \frac{\partial U_z}{\partial x} = \left(1 - \frac{4z^2}{h^2}\right)\left(\phi_x + \frac{\partial u_z}{\partial x}\right), && \tau_{xz} = G\gamma_{xz}, \\
\gamma_{yz} &= \frac{\partial U_y}{\partial z} + \frac{\partial U_z}{\partial y} = \left(1 - \frac{4z^2}{h^2}\right)\left(\phi_y + \frac{\partial u_z}{\partial y}\right), && \tau_{yz} = G\gamma_{yz}.
\end{aligned} \tag{20}$$

3.2. Stress resultants and equilibrium equations

By the aid of Eq. (20), the calculation of the stress resultants in Eq. (2) leads to

$$M_x = D\left(\frac{\partial\phi_x}{\partial x} + \nu\frac{\partial\phi_y}{\partial y}\right) - \frac{Dh^2}{40}\left(\frac{2-\nu}{1-2\nu}\right)\left[(1-\nu)\frac{\partial^2}{\partial x^2} + \nu\frac{\partial^2}{\partial y^2}\right]\left(\frac{\partial\phi_x}{\partial x} + \frac{\partial\phi_y}{\partial y}\right), \tag{21}$$

$$M_y = D\left(\nu\frac{\partial\phi_x}{\partial x} + \frac{\partial\phi_y}{\partial y}\right) - \frac{Dh^2}{40}\left(\frac{2-\nu}{1-2\nu}\right)\left[(1-\nu)\frac{\partial^2}{\partial y^2} + \nu\frac{\partial^2}{\partial x^2}\right]\left(\frac{\partial\phi_x}{\partial x} + \frac{\partial\phi_y}{\partial y}\right), \tag{22}$$

$$M_{xy} = \frac{D}{2}(1-\nu)\left(\frac{\partial\phi_x}{\partial y} + \frac{\partial\phi_y}{\partial x}\right) - \frac{Dh^2}{40}(2-\nu)\frac{\partial^2}{\partial x\partial y}\left(\frac{\partial\phi_x}{\partial x} + \frac{\partial\phi_y}{\partial y}\right), \tag{23}$$

$$Q_x = \frac{2}{3}Gh\left(\phi_x + \frac{\partial u_z}{\partial x}\right), \tag{24}$$

$$Q_y = \frac{2}{3}Gh\left(\phi_y + \frac{\partial u_z}{\partial y}\right), \tag{25}$$

where

$$D = \frac{Eh^3}{12(1-\nu^2)} \quad \text{with} \quad E = 2G(1+\nu). \tag{26}$$

The equilibrium equations for the interior plate are obtained as follows. After integrated with respect to the thickness coordinate z, the stress equilibrium equations obtained by considering the stresses acting on an infinitesimal parallelepiped element take the form (see, Vinson, 2006)

$$\frac{\partial M_x}{\partial x} + \frac{\partial M_{xy}}{\partial y} = Q_x, \quad \frac{\partial M_y}{\partial y} + \frac{\partial M_{xy}}{\partial x} = Q_y, \quad \frac{\partial Q_x}{\partial x} + \frac{\partial Q_y}{\partial y} = 0. \tag{27}$$

3.3. Uniform distributed load

In lack of a suitable general solution for pressure loading, only the solution of the homogeneous problem ($p = 0$) was considered above. However, to elucidate some features related to loaded plates in the next section, we consider a particular solution for a uniformly distributed load $p = p_0$ acting on the upper face of the plate (see Fig. 1). Piltner's (1992a) solution for such a load is

$$2G \cdot U_x = \frac{p_0 x}{4h^3}\left[(2-\nu)(4z^3 - 3h^2 z) - 3(1-\nu)(x^2+y^2)z + \frac{2\nu h^2}{1+\nu}\right], \tag{28}$$

$$2G \cdot U_y = \frac{p_0 y}{4h^3}\left[(2-\nu)(4z^3 - 3h^2 z) - 3(1-\nu)(x^2+y^2)z + \frac{2\nu h^2}{1+\nu}\right], \tag{29}$$

$$\begin{aligned} 2G \cdot U_z = \frac{p_0}{16h^3}\Bigg[&24\nu(x^2+y^2)z^2 - 8(1+\nu)z^4 + 12h^2(1+\nu)z^2 \\ &+ 3(1-\nu)(x^2+y^2)^2 - 6h^2\nu(x^2+y^2) - \frac{8h^3}{1+\nu}z\Bigg]. \end{aligned} \tag{30}$$

In order to study interior plates under uniform pressure, the 3D displacements given by Eqs. (28)–(30) are added to the homogeneous solution given by Eqs. (6)–(8). The particular solution then contributes to the mid-surface variables (10) by polynomials (see Appendix A). We note that the uniform load adds to the right-hand side of displacement U_z given by Eq. (15) the term

$$U_z^p = -\frac{p_0 z}{4Eh^3}\left(\frac{1+\nu}{1-\nu}\right)\left[(2-4\nu)h^3 - (3-6\nu)h^2 z + 2(1-\nu^2)z^3\right], \tag{31}$$

whereas Eqs. (13) and (14) retain their forms. In addition, the right-hand side of Eq. $(27)_3$ changes so that 0 is substituted by $-p_0$.

3.4. Connection to approximate theories

Finally, we take a look at how the Kirchhoff, Mindlin (1951) and Levinson (1980) plate theories are related to the presented elasticity-based 2D plate theory. Membrane contributions are not considered. The equilibrium equations (27) hold for all theories. If we neglect the Poisson effect ($\nu = 0$) in the displacements (13)–(15), the displacement field is exactly of the same form as that used by Levinson (1980) and Reddy (1984). Furthermore, when the third-order contributions z^3 are eliminated, the kinematic description for the Mindlin plate theory is obtained. Finally, in the limit $h \to 0$, Eqs. (11) give $\phi_x = -\partial u_z/\partial x$ and $\phi_y = -\partial u_z/\partial y$, which bring us to the Kirchhoff plate theory. Comparison between the strains and stresses is best done through the stress resultants. By neglecting the higher-order contributions in Eqs. (21)–(25), the stress resultants of the Mindlin plate theory with the shear coefficient $\kappa = 2/3$ are obtained. Furthermore, by setting $h = 0$, but retaining Eq. (26), the moments of the Kirchhoff plate theory are obtained.

We study the equilibrium equations (27) of the plates in terms of the mid-surface variables, see Eqs. (A.1). The homogeneous case yields $\nabla^4 u_z = 0$, but with the constant load included, we obtain the relation

$$D\nabla^4 u_z = -p_0, \tag{32}$$

which is the same as the differential equation for the transverse deflection of a Kirchhoff plate subjected to a uniformly distributed load. *However, the most remarkable aspect in this comparison between the different plate theories is that the elasticity solution (6)–(8) is also a general homogeneous solution to the Mindlin and Levinson plate equations.* To elaborate on this, Levinson's equations for a plate under a uniformly distributed load as the particular contribution can be written as (Levinson, 1980)

$$\frac{2D}{5}\left[(1-\nu)\nabla^2\phi_x + (1+\nu)\frac{\partial}{\partial x}\left(\frac{\partial \phi_x}{\partial x} + \frac{\partial \phi_y}{\partial y}\right) - \frac{1}{2}\frac{\partial}{\partial x}\nabla^2 u_z\right] = \frac{2}{3}Gh\left(\phi_x + \frac{\partial u_z}{\partial x}\right), \tag{33}$$

$$\frac{2D}{5}\left[(1-\nu)\nabla^2\phi_y + (1+\nu)\frac{\partial}{\partial y}\left(\frac{\partial \phi_x}{\partial x} + \frac{\partial \phi_y}{\partial y}\right) - \frac{1}{2}\frac{\partial}{\partial y}\nabla^2 u_z\right] = \frac{2}{3}Gh\left(\phi_y + \frac{\partial u_z}{\partial y}\right), \tag{34}$$

$$\frac{2}{3}Gh\left(\nabla^2 u_z + \frac{\partial \phi_x}{\partial x} + \frac{\partial \phi_y}{\partial y}\right) = -p_0, \tag{35}$$

It is easy to verify that Eqs. (33)–(35) are satisfied by Eqs. (A.1). We obtain Mindlin's plate equations from Eqs. (33)–(35) by the replacements $2D/5 \to D/2$ and $(2/3)Gh \to \kappa Gh$ and by neglecting the term $\nabla^2 u_z$ in Eqs. (33) and (34). In the dynamic case, Levinson (1980) showed that his equations were equivalent to Mindlin's for $\kappa = 5/6$. Further comparisons between the discussed plate theories are provided in Section 5 by using the same mid-surface solution for all shear deformation theories. In order to calculate and compare the stresses, the mid-surface variables are expanded according to the 3D displacement field of each shear deformation theory.

In their study on boundary layers and interior equations for plates, Nosier and Reddy (1992) showed that the governing equations of the Mindlin and Levinson plate theories may be presented in terms of a second-order edge-zone equation and a fourth-order interior equation. Their potential function describing the edge-zone was defined as $\Phi = \partial\phi_x/\partial y - \partial\phi_y/\partial x$. However, in the isotropic case we have $\partial\phi_x/\partial y = \partial\phi_y/\partial x$ according to Eq. $(12)_1$ and, thus, the edge-zone potential vanishes ($\Phi = 0$). In conclusion, the linearly elastic, isotropic, homogeneous Kirchhoff, Mindlin and Levinson plate theories are interior theories, as will be demonstrated further in the next sections.

4. Variational interior formulation of the Levinson plate theory

In this section, we carry out a variational interior formulation for the Levinson plate theory to shed light on 2D engineering plate theories from an energetical point of view. The formulation is based on the principle of virtual displacements and accounts for the virtual work done by the interior stresses acting as surface tractions on the lateral edges of the plate. By employing the obtained natural interior boundary conditions, higher-order stress resultants are eliminated from the equilibrium equations. Variational interior formulations for a Levinson beam and circular plates have been presented earlier by Karttunen and von Hertzen (2015, 2016b). In light of this, we note that the current derivation extends the variational interior framework from 1D to 2D systems.

4.1. Equilibrium equations and interior boundary conditions

In the following formulation of the Levinson plate theory we assume that the mid-surface variables $u_z(x,y)$, $\phi_x(x,y)$ and $\phi_y(x,y)$ are sufficiently smooth but otherwise arbitrary functions. For the sake of brevity, we write the kinematic description of the rectangular Levinson plate (1980) in the form

$$U_x = z\phi_x - \alpha z^3\left(\phi_x + u_{z,x}\right), \tag{36}$$

$$U_y = z\phi_y - \alpha z^3\left(\phi_y + u_{z,y}\right), \tag{37}$$

$$U_z = u_z. \tag{38}$$

where $\alpha = 4/3h^2$, and x and y in the subscripts after the comma denote partial differentiation with respect to coordinates x and y, respectively. Assuming plane stress constitutive relations ($\sigma_z = 0$), the nonzero strains and stresses calculated using the displacements (36)–(38) are

$$\begin{aligned}
\epsilon_x &= z\phi_{x,x} - \alpha z^3(\phi_{x,x} + u_{z,xx}), & \sigma_x &= \frac{E}{1-\nu^2}\left(\epsilon_x + \nu\epsilon_y\right),\\
\epsilon_y &= z\phi_{y,y} - \alpha z^3(\phi_{y,y} + u_{z,yy}), & \sigma_y &= \frac{E}{1-\nu^2}\left(\nu\epsilon_x + \epsilon_y\right),\\
\gamma_{xy} &= z\left(\phi_{x,y} + \phi_{y,x}\right) - \alpha z^3\left(\phi_{x,y} + \phi_{y,x} + 2u_{z,xy}\right), & \tau_{xy} &= G\gamma_{xy},\\
\gamma_{xz} &= \left(1 - 3\alpha z^2\right)\left(\phi_x + u_{z,x}\right), & \tau_{xz} &= G\gamma_{xz},\\
\gamma_{yz} &= \left(1 - 3\alpha z^2\right)\left(\phi_y + u_{z,y}\right), & \tau_{yz} &= G\gamma_{yz}.
\end{aligned} \tag{39}$$

The internal virtual work (virtual strain energy) of the plate is

$$\begin{aligned}
\delta U &= \int_V (\sigma_x\delta\epsilon_x + \sigma_y\delta\epsilon_y + \tau_{xy}\delta\gamma_{xy} + \tau_{xz}\delta\gamma_{xz} + \tau_{yz}\delta\gamma_{yz})dV\\
&= \int_{-b}^{b}\int_{-a}^{a}\Big[M_x\delta\phi_{x,x} + M_y\delta\phi_{y,y} + M_{xy}\left(\delta\phi_{x,y} + \delta\phi_{y,x}\right)\\
&- \alpha P_x\left(\delta\phi_{x,x} + \delta u_{z,xx}\right) - \alpha P_y\left(\delta\phi_{y,y} + \delta u_{z,yy}\right) - \alpha P_{xy}\left(\delta\phi_{x,y} + \delta\phi_{y,x} + 2\delta u_{z,xy}\right)\\
&+ \left(Q_x - 3\alpha R_x\right)\left(\delta\phi_x + \delta u_{z,x}\right) + \left(Q_y - 3\alpha R_y\right)\left(\delta\phi_y + \delta u_{z,y}\right)\Big]dxdy,
\end{aligned} \tag{40}$$

where the classical stress resultants read

$$M_x = \int_{-h/2}^{h/2} \sigma_x z dz = \frac{D}{5}\left[4\left(\phi_{x,x} + \nu\phi_{y,y}\right) - \left(u_{z,xx} + \nu u_{z,yy}\right)\right], \tag{41}$$

$$M_y = \int_{-h/2}^{h/2} \sigma_y z dz = \frac{D}{5}\left[4\left(\nu\phi_{x,x} + \phi_{y,y}\right) - \left(\nu u_{z,xx} + u_{z,yy}\right)\right], \tag{42}$$

$$M_{xy} = \int_{-h/2}^{h/2} \tau_{xy} z dz = \frac{D}{5}\left(\frac{1-\nu}{2}\right)\left[4\left(\phi_{x,y} + \phi_{y,x}\right) - 2u_{z,xy}\right], \tag{43}$$

$$Q_x = \int_{-h/2}^{h/2} \tau_{xz} dz = \frac{2}{3} Gh\left(\phi_x + u_{z,x}\right), \tag{44}$$

$$Q_y = \int_{-h/2}^{h/2} \tau_{yz} dz = \frac{2}{3} Gh\left(\phi_y + u_{z,y}\right) \tag{45}$$

and the higher-order stress resultants are

$$P_x = \int_{-h/2}^{h/2} \sigma_x z^3 dz = \frac{Dh^2}{140}\left[16\left(\phi_{x,x} + \nu\phi_{y,y}\right) - 5\left(u_{z,xx} + \nu u_{z,yy}\right)\right], \tag{46}$$

$$P_y = \int_{-h/2}^{h/2} \sigma_y z^3 dz = \frac{Dh^2}{140}\left[16\left(\nu\phi_{x,x} + \phi_{y,y}\right) - 5\left(\nu u_{z,xx} + u_{z,yy}\right)\right], \tag{47}$$

$$P_{xy} = \int_{-h/2}^{h/2} \tau_{xy} z^3 dz = \frac{Dh^2}{70}\left(\frac{1-\nu}{2}\right)\left[8\left(\phi_{x,y} + \phi_{y,x}\right) - 5u_{z,xy}\right], \tag{48}$$

$$R_x = \int_{-h/2}^{h/2} \tau_{xz} z^2 dz = \frac{Gh^3}{30}\left(\phi_x + u_{z,x}\right), \tag{49}$$

$$R_y = \int_{-h/2}^{h/2} \tau_{yz} z^2 dz = \frac{Gh^3}{30}\left(\phi_y + u_{z,y}\right). \tag{50}$$

The external virtual work due to the interior stresses acting as surface tractions on the lateral edges of the plate is calculated using Eqs. (5). As an example, according to the positive and negative directions of the displacements and stresses (see Fig. 2), the virtual work contribution by the normal stress σ_x on edges $x = \pm a$ is as follows

$$\int_{-b}^{b}\int_{-h/2}^{h/2}(\underbrace{+\sigma_x \delta U_x}_{(+a,y,z)} \underbrace{-\sigma_x \delta U_x}_{(-a,y,z)}) dz dy = \int_{-b}^{b}\left[(M_x - \alpha P_x)\delta\phi_x - \alpha P_x \delta u_{z,x}\right]_{-a}^{a} dy. \tag{51}$$

The full expression for the external virtual work due to the interior stresses is

$$\begin{aligned}\delta W_s = &\int_{-b}^{b}\left[(M_x - \alpha P_x)\delta\phi_x - \alpha P_x \delta u_{z,x} + (M_{xy} - \alpha P_{xy})\delta\phi_y - \alpha P_{xy}\delta u_{z,y} + Q_x \delta u_z\right]_{-a}^{a} dy \\ + &\int_{-a}^{a}\left[(M_y - \alpha P_y)\delta\phi_y - \alpha P_y \delta u_{z,y} + (M_{xy} - \alpha P_{xy})\delta\phi_x - \alpha P_{xy}\delta u_{z,x} + Q_y \delta u_z\right]_{-b}^{b} dx.\end{aligned} \tag{52}$$

By applying the principle of virtual displacements, $\delta U = \delta W_s$, we arrive at the following intermediate equilibrium equations

$$M_{x,x} + M_{xy,y} - Q_x = \alpha\left(P_{x,x} + P_{xy,y} - 3R_x\right), \tag{53}$$
$$M_{y,y} + M_{xy,x} - Q_y = \alpha\left(P_{y,y} + P_{xy,x} - 3R_y\right), \tag{54}$$
$$Q_{x,x} + Q_{y,y} = -\alpha\left[P_{x,xx} + 2P_{xy,xy} + P_{y,yy} - 3\left(R_{x,x} + R_{y,y}\right)\right]. \tag{55}$$

By combining the boundary terms of Eq. (52) with those produced by integration by parts of Eq. (40) we obtain

$$\left[\alpha\left(P_{x,x} + P_{xy,y} - 3R_x\right)\delta u_z\right]_{-a}^{a} = 0, \tag{56}$$
$$\left[\alpha\left(P_{y,y} + P_{xy,x} - 3R_y\right)\delta u_z\right]_{-b}^{b} = 0. \tag{57}$$

Consequently, we require that the virtual displacement δu_z or the expressions multiplying it above must vanish at the edges. It follows from the interior problem definition in Section 2 that the virtual displacement δu_z is free in the whole interior plate region. Therefore, the (natural) interior boundary conditions become

$$\alpha\left(P_{x,x} + P_{xy,y} - 3R_x\right)(\pm a, y) = 0, \tag{58}$$
$$\alpha\left(P_{y,y} + P_{xy,x} - 3R_y\right)(x, \pm b) = 0. \tag{59}$$

At this point, it may be verified that the equilibrium equations (53)–(55) and the interior boundary conditions (58) and (59) are satisfied by Eqs. (10). That is to say, the variational formulation is in line with the general 3D interior elasticity problem and its solution. Note that a variational formulation equivalent to the above could be carried out by adhering to Clapeyron's theorem $C = 2U - W_s = 0$ so that $\delta C = 0$. This way the importance of the virtual work contribution (52) becomes more apparent because one sees that the strain energy needs to be balanced by the surface tractions for the formulation to be on a nontrivial basis.

4.2. Elimination of higher-order stress resultants

We introduce the following two variables

$$f_1(x, y) = \alpha\left(P_{x,x} + P_{xy,y} - 3R_x\right), \tag{60}$$
$$f_2(x, y) = \alpha\left(P_{y,y} + P_{xy,x} - 3R_y\right). \tag{61}$$

Now the interior boundary conditions (58) and (59) can be written in the form

$$f_1(\pm a, y) = 0, \tag{62}$$
$$f_2(x, \pm b) = 0, \tag{63}$$

respectively. Moreover, using Eqs. (44), (49), (53) and (60) we can write

$$f_1 = -\frac{D}{210}\left[2(u_{z,xxx} + u_{z,xyy}) + 2\phi_{x,xx} + (1-\nu)\phi_{x,yy} + (1+\nu)\phi_{y,xy}\right]. \tag{64}$$

Furthermore, by the aid of Eqs. (45), (50), (54) and (61), we obtain

$$f_2 = -\frac{D}{210}\left[2(u_{z,yyy} + u_{z,xxy}) + 2\phi_{y,yy} + (1-\nu)\phi_{y,xx} + (1+\nu)\phi_{x,xy}\right]. \tag{65}$$

On the other hand, a look at the equilibrium equations (53)–(55) and shear forces (44) and (45) gives us

$$f_{1,x} + f_{2,y} = -Q_{x,x} - Q_{y,y} = -\frac{2}{3} Gh \left(\phi_{x,x} + \phi_{y,y} + u_{z,xx} + u_{z,yy}\right). \tag{66}$$

By applying relation $(12)_1$ ($\phi_{x,y} = \phi_{y,x}$), which stems from the general solution, to Eqs. (64) and (65) and taking into account Eq. (66), we arrive at the coupled partial differential equations

$$f_{1,xx} + f_{2,xy} - \beta^2 f_1 = 0, \tag{67}$$

$$f_{2,yy} + f_{1,xy} - \beta^2 f_2 = 0, \tag{68}$$

where

$$\beta^2 = 70\frac{Gh}{D} = \frac{420(1-\nu)}{h^2} \tag{69}$$

We consider our solution to Eqs. (67) and (68) to be of the separable form

$$f_1 = X_1(x)Y_1(y), \tag{70}$$

$$f_2 = X_2(x)Y_2(y). \tag{71}$$

Now Eqs. (67) and (68) can be written as

$$\left(\frac{X_{1,xx}}{X_1} - \beta^2\right)\frac{X_1}{X_{2,x}} = -\frac{Y_{2,y}}{Y_1} = \alpha_1^2, \tag{72}$$

$$\left(\frac{Y_{2,yy}}{Y_2} - \beta^2\right)\frac{Y_2}{Y_{1,y}} = -\frac{X_{1,x}}{X_2} = \alpha_2^2, \tag{73}$$

where α_1 and α_2 are nonzero constants. Furthermore, we have

$$X_{1,xx} - \zeta_1^2 X_1 = 0, \tag{74}$$

$$Y_{2,yy} - \zeta_2^2 Y_2 = 0, \tag{75}$$

where

$$\zeta_1^2 = \frac{\beta^2\alpha_2^2}{\alpha_1^2 + \alpha_2^2} \quad \text{and} \quad \zeta_2^2 = \frac{\beta^2\alpha_1^2}{\alpha_1^2 + \alpha_2^2}. \tag{76}$$

The general solutions to Eqs. (74) and (75) are

$$X_1(x) = A_1 \mathrm{e}^{\zeta_1 x} + A_2 \mathrm{e}^{-\zeta_1 x}, \tag{77}$$

$$Y_2(y) = B_1 \mathrm{e}^{\zeta_2 y} + B_2 \mathrm{e}^{-\zeta_2 y}, \tag{78}$$

respectively. By using the separated forms (70) and (71), the interior boundary conditions (62) and (63) become

$$X_1(\pm a)Y_1(y) = 0 \to X_1(a) = X_1(-a) = 0, \tag{79}$$

$$X_2(x)Y_2(\pm b) = 0 \to Y_2(b) = Y_2(-b) = 0. \tag{80}$$

Application of the above boundary conditions to Eqs. (77) and (78) gives us $X_1(x) = 0$ and $Y_2(y) = 0$ (for all separable solutions), which through Eqs. (70) and (71) lead to

$$\underline{\underline{f_1(x,y) = f_2(x,y) = 0}}. \tag{81}$$

Substitution of result (81) into the equilibrium equations (53)–(55) gives

$$M_{x,x} + M_{xy,y} = Q_x, \quad M_{y,y} + M_{xy,x} = Q_y, \quad Q_{x,x} + Q_{y,y} = 0, \tag{82}$$

which are the same as Eqs. (27), but are repeated here for the sake of completeness.

4.3. Remarks on variational formulations

The above result (82), which implies that the Levinson plate equilibrium equations are always ultimately of the given form, is merely a manifestation of the fact that the differences between Newtonian and Lagrangian approaches are mathematical, not physical. The equilibrium equations (53)–(55) containing higher-order stress resultants are meaningful only if they are associated with the interior boundary conditions (58) and (59). The boundary conditions eliminate artificial, exponentially decaying edge effects kin to those seen in Eqs. (77) and (78), or equivalently, they rid us of the higher-order stress resultants. The correct interior boundary conditions (58) and (59) are obtained only if the virtual work contribution (52) due to the interior stresses is accounted for.

A large number of different displacement-based third- and other higher-order plate theories can be found in the literature. For a recent comprehensive listing, see the paper by Nguyen et al. (2016). A typical variational formulation of a higher-order 2D plate theory is based on a displacement field that satisfies stress-free face conditions but makes no reference to the lateral boundaries of the plate. Such a field is exclusively an interior field. Furthermore, virtually all engineering plate formulations adhere to Saint Venant's principle not only by using an interior kinematic description for the whole plate but also by relying on stress resultants instead of detailed stress distributions on the plate edges so that physically plausible edge effects are eliminated. However, because the work done by the interior stresses acting as surface tractions on the lateral plate edges is usually not accounted for in energy-based formulations of higher-order theories, the derived equations produce artificial edge effects which reside in a boundary layer built upon interior displacements. In short, a flaw in the formulation materializes as a logical fallacy in the end result. If a proper boundary layer is desired, the elasticity solutions for linearly elastic, isotropic, homogeneous plates that deal with Papkovich-Fadle functions may be used as the starting point, see the work of Piltner (1992a).

Nevertheless, all higher-order engineering plate theories are not completely without merit. It is well-known that they provide good results for many practical problems far enough from the lateral plate edges regardless of their variational crimes chaining them to artificial edge effects. However, the higher-order theories are unnecessarily complicated in comparison to the theory by Levinson because when the external virtual work due to the interior stresses is not accounted for in a variational formulation, the total differential order of the resulting governing equations increases, as suggested by the exponential functions describing the artificial boundary behavior, cf. Eqs. (74)–(78). For the application of the simple Levinson plate theory, see the works of Levinson and Cooke (1983; 1983), Bert (1984) and Reddy et al. (2001) in addition to Levinson (1980).

Finally, we note again that the Levinson plate does not have a boundary layer and, thus, a variational formulation does not produce any more information than a vectorial formulation on how to apply boundary conditions in practical engineering problems. Interestingly, if a variational interior formulation is carried out for a Mindlin plate, not even the interior boundary conditions (cf. Eqs. (56) and (57)) appear in the theory because the boundary terms that stem from the virtual strain energy and the external virtual work cancel each other completely and the equilibrium equations are automatically of the correct form (82). The conditions on the edges of an interior plate may be chosen only so as to imitate true, pointwise boundary conditions. This is the standard practice also in the context of 2D linear elasticity when interior plane beam problems are studied using Airy stress functions (see, Timoshenko and Goodier, 1970). Methods to determine optimal boundary conditions for elasticity-based plates have been studied by Gregory and Wan (1985) and Barrett and Ellis (1988). However, in the next section the application of constraints on the edges of interior plates in practical plate problems is done in a more straightforward manner.

5. Case studies from Clapeyron to plate bending

Motivated by the fact that the particular solution (28)–(30) for the uniform load is given in polynomial form, the biharmonic function Ψ in the homogeneous solution (6)–(8) for our calculation examples that consider the accuracy of the discussed interior plate theories is taken to be a polynomial of the form

$$\begin{aligned}\Psi(x,y) = {} & c_1 + c_2x + c_3y + c_4x^2 + c_5xy + c_6y^2 + c_7x^3 + c_8y^3 + c_9x^2y + c_{10}xy^2 \\ & + c_{11}x^3y + c_{12}xy^3 + c_{13}(x^4 - 3x^2y^2) + c_{14}(y^4 - 3x^2y^2) + c_{15}(x^5 - 5x^3y^2) \\ & + c_{16}(y^5 - 5x^2y^3) + c_{17}(x^4y - x^2y^3) + c_{18}(xy^4 - x^3y^2) + P(x,y),\end{aligned} \tag{83}$$

where $P(x,y)$ includes higher-order biharmonic polynomials and is given in Appendix B. By using Eq. (83), it is easy to verify that the full general solution, which is the sum of the homogeneous (6)–(8) and particular (28)–(30) contributions, satisfies Clapeyron's theorem, that is,

$$\underline{\underline{2U - W_s - W_p = 0}}\,, \tag{84}$$

where U and W_s are given by Eqs. (4) and (5), and the work due to the uniform load is

$$W_p = -\int_{-b}^{b}\int_{-a}^{a} \sigma_z(x,y,-h/2)U_z(x,y,-h/2)dxdy = \int_{-b}^{b}\int_{-a}^{a} p_0U_z(x,y,-h/2)dxdy. \tag{85}$$

The Levinson plate (1980) also satisfies Eq. (84) when Eqs. (A.1) with (83) are used. To summarize our energy considerations, when interior equations are derived in a Newtonian way, the total potential energy is captured as a by-product, whereas a Lagrangian approach requires that each work and energy contribution, some of which may be elusive, is individually accounted for.

In the following we study mainly rectangular plates subjected to a uniformly distributed load. The biharmonic polynomial in Eq. (83) includes forty-eight arbitrary constants to be determined from constraint conditions set at a limited number of points along the plate edges. The acquired plate solutions are exact in the sense that they satisfy the interior stress boundary conditions (Section 2) and the Navier equations of elasticity. Although the solutions are not complete, forty-eight constants are enough to obtain very accurate results for many cases. To facilitate the use of solutions (6)–(8) and (28)–(30), a supplementary Mathematica file *Simply48* is provided online (see the end of the Manuscript for PDF version). The file solves the case of a simply-supported plate under a uniform load presented in Section 5.3 using the biharmonic polynomial of Eq. (83).

5.1. All edges clamped

As our first example, we study a square plate with all of its four edges clamped. In order to solve the arbitrary constants in Eq. (83), we form the constraint conditions $u_z = \phi_x = \phi_y = 0$ in the plate corners and at equally spaced points along the plate edges using Eqs. (A.1). For numerical calculations, the parameter values are taken to be the same as those used by Piltner (1992b). In more detail, we have $a = b = 5$, $h = 0.01$, $E = 10.92$, $\nu = 0.3$ and $p_0 = 1$. Figure 3 shows the transverse deflection $u_z(x,y)$ on the mid-surface for two different cases. In Fig. 3(a), the first twenty-four terms of the polynomial in Eq. (83) have been used to clamp the plate at eight points, including the plate corners, whereas in Fig. 3(b) all forty-eight terms have been used to enforce the displacement constraints at sixteen equally spaced points. In Fig. 3(a), we can see that the plate edges display a waviness suggesting that eight points are not enough to clamp the plate

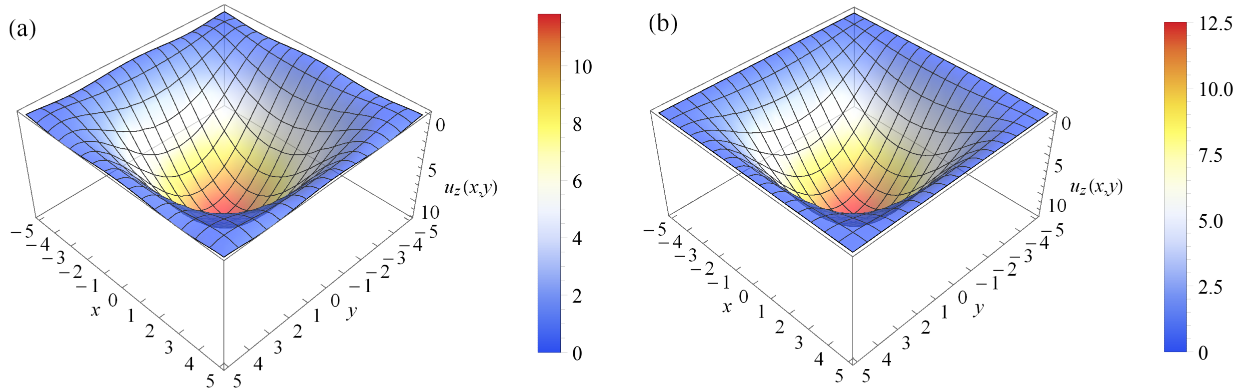

Figure 3: Transverse deflection on the mid-surface of a square plate under a uniform load with all edges clamped using a) 24 first terms of the biharmonic polynomial (83) and b) all 48 terms.

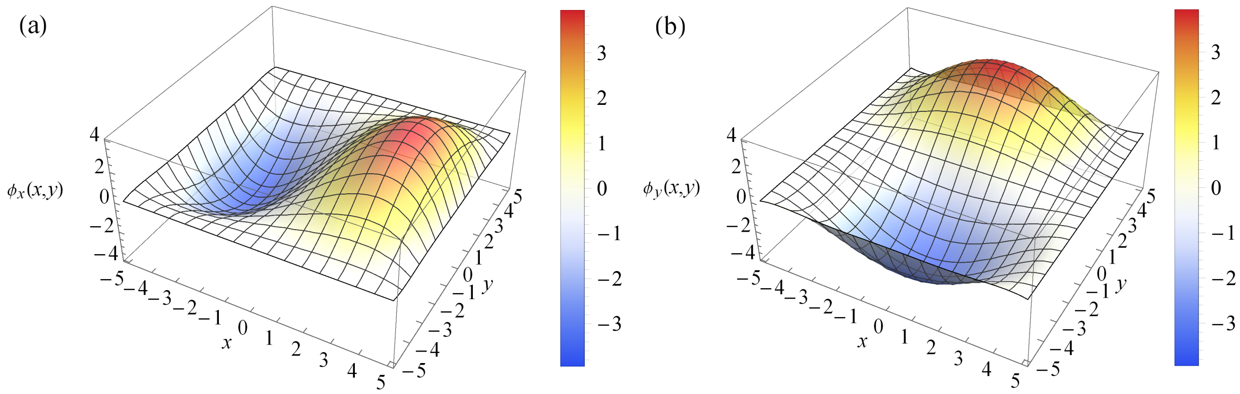

Figure 4: Rotations a) ϕ_x and b) ϕ_y on the mid-surface of a square plate under a uniform load with all edges clamped using the polynomial (83) with 48 terms.

properly. By doubling the number of constraint points, a notable improvement in clamping the plate is achieved as indicated by Fig. 3(b). Figure 4 shows the rotation variables on the mid-surface calculated using the full polynomial in Eq. (83). We see that the rotations are zero along the edges.

An analytical series solution can be obtained for a Kirchhoff plate with all edges clamped (Timoshenko and Woinowsky-Krieger, 1959). The series solution can be viewed as an exact elasticity solution for a thin plate because the Kirchhoff theory is a special case of the exact interior elasticity solution at hand [cf. Eq. (32)]. With the current parameter values the maximum deflection given by the series solution is $u_z = 12.64$ (Piltner, 1992b), whereas the polynomial in Eq. (83) leads to $u_z = 11.84$ and $u_z = 12.66$ for the cases in Figs. 3(a) and 3(b), respectively. In conclusion, the series solution and the polynomial in Eq. (83) with all its forty-eight terms accounted for give practically the same result and, thus, the polynomial approach satisfying constraint conditions only at a rather limited number of points is found valid in this case.

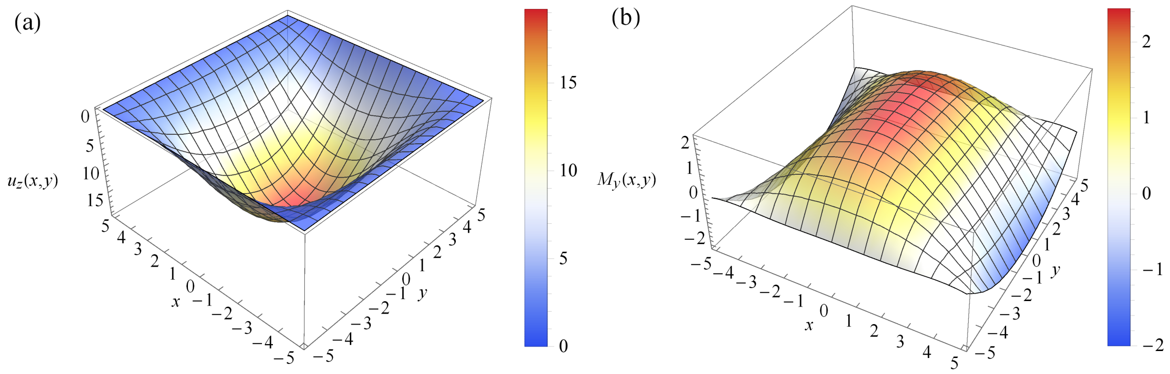

Figure 5: a) Transverse deflection on the mid-surface of a square plate under a uniform load with two opposite edges simply-supported ($y = \pm b$) and the other two clamped ($x = \pm a$). b) Moment M_y of the same plate.

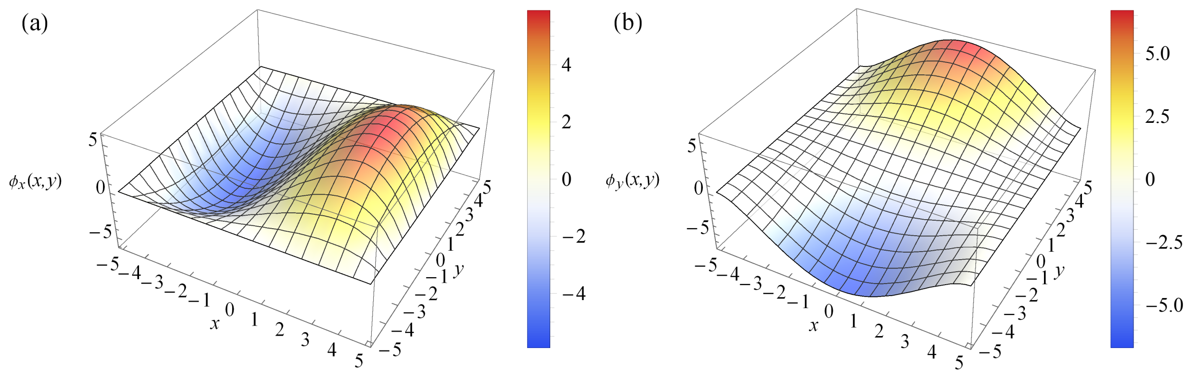

Figure 6: Rotations a) ϕ_x and b) ϕ_y on the mid-surface of a square plate under a uniform load with two opposite edges simply-supported ($y = \pm b$) and the other two clamped ($x = \pm a$).

5.2. Two edges simply-supported, two clamped

Next we take a look at a plate with two opposite edges simply-supported and the other two clamped. The full polynomial in Eq. (83) with forty-eight constants is used. For the clamped edges $x = \pm a$ we have the conditions $u_z = \phi_x = \phi_y = 0$, whereas for the simply-supported edges $y = \pm b$ we use $u_z = \phi_x = M_y = 0$. The corner conditions are not without some ambiguity. In more detail, we may choose either $\phi_y = 0$ or $M_y = 0$ for each corner in addition to $u_z = \phi_x = 0$. Using the same parameter values as in the previous example, we obtain for the maximum displacement at the plate center $u_z = 19.176$ and $u_z = 19.178$ for the former and latter cases, respectively. The well-known series solution for a Kirchhoff plate gives $u_z = 19.2$ (Timoshenko and Woinowsky-Krieger, 1959). The differences between the three solutions are nominal. In Fig. 5, we have chosen to use the conditions $u_z = \phi_x = \phi_y = 0$ in the corners. It seems more straightforward to set only displacements constraints in the corners instead of a mixed set of displacements and a moment. Figure 5(a) displays the transverse deflection of the plate on the mid-surface and Fig. 5(b) shows the distribution of moment M_y. Figures 6(a) and 6(b) present rotations ϕ_x and ϕ_y on the mid-surface, respectively. Figs. 5 and 6 indicate that the constraint conditions are fulfilled satisfactorily.

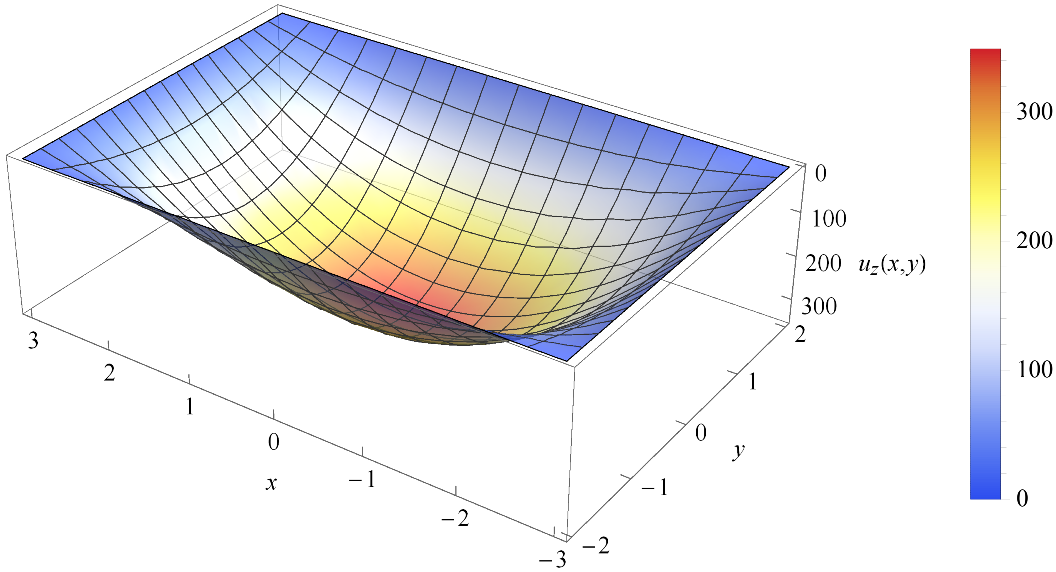

Figure 7: Transverse deflection on the mid-surface of a simply-supported rectangular plate under a uniform load using the biharmonic polynomial in Eq. (83) with 48 arbitrary constants.

5.3. All edges simply-supported

As a more comprehensive example we study a simply-supported plate under a uniform load. The parameter values are taken from the work of Piltner (1992b). In this case, we have $a = 3$, $b = 2$, $E = 1$, $\nu = 0.3$ and $p_0 = 1$. The thickness of the plate is varied in the calculations. The obtained results are compared to those of Piltner (1988, 1992b). As already mentioned, the calculations and additional figures for the studied case are given in the Supplementary online Mathematica file *Simply48* provided both in NB and PDF formats. Figure 7 shows the transverse deflection on the mid-surface of the plate for $h = 0.4$. In addition to the corner constraints $u_z = \phi_x = \phi_y = 0$, we have used the conditions $u_z = \phi_y = M_x = 0$ for edges $x = \pm a$ and $u_z = \phi_x = M_y = 0$ for edges $y = \pm b$.

Table 1 and Fig. 8(a) show a comparison between the present solution and Piltner's exact 3D solution (1988; 1992b) in terms of maximum transverse deflections for different plate thicknesses. In Fig. 8(a) the relative difference between the solutions is calculated from

$$\Delta u_{z,\mathrm{rel}} = 100 \times \frac{u_{z,\mathrm{Piltner}} - u_{z,\mathrm{Present}}}{u_{z,\mathrm{Present}}}\,. \tag{86}$$

Figure 8(a) shows that the differences between Piltner's exact 3D solution and the present solution (48 constants) are very small ($0.1\% - 0.3\%$). When only the first twenty-four terms are accounted for in Eq. (83), the differences are larger.

The stresses of the Mindlin, Levinson and the exact interior plates are studied in Table 1 and Fig. 8(b). Although the mid-surface displacement solution based on Eqs. (A.1) is the same for all three cases as discussed in Section 3.4, the differences between the plates become evident by a closer look at stress σ_x at point $(0, 0, -h/2)$. Figure 8(b) shows the relative differences between Piltner's exact 3D solution and the other ones. For thin plates the differences are small but as

Table 1: Comparison of displacements and stresses between different solutions. Stresses for the Mindlin and Levinson plates were calculated by expanding the exact mid-surface solution (48 constants) through the plate thickness according to the respective kinematic and constitutive assumptions of the Mindlin and Levinson plates.

	24 const.	48 const.	Piltner	Mindlin	Levinson	Present	Piltner (1992b)
h	$u_z(0,0)$	$u_z(0,0)$	$u_z(0,0)$	$\sigma_x(0,0,-h/2)$	$\sigma_x(0,0,-h/2)$	$\sigma_x(0,0,-h/2)$	$\sigma_x(0,0,-h/2)$
0.1	21471	21662	21637	-478.3	-478.5	-478.5	-479.0
0.2	2703.2	2724.9	2721.4	-119.6	-119.7	-119.8	-120.0
0.4	347.50	349.05	348.53	-29.90	-30.03	-30.10	-30.27
0.6	107.62	107.56	107.38	-13.29	-13.42	-13.50	-13.66
0.8	48.109	47.814	47.721	-7.474	-7.607	-7.683	-7.845
1.0	26.393	26.086	26.016	-4.783	-4.917	-4.993	-5.153

the plate thicknesses increase, so do the differences. The present exact plate takes into account only the interior bending solution, whereas Piltner's exact 3D solution is not exclusively an interior solution. As Piltner's plate becomes thicker, interior bending no longer dominates in his solution, that is, the boundary layer solution also starts to play a role. In other words, the differences between the present interior-only solution and Piltner's full solution increase for thicker plates due to the presence of the boundary layer in Piltner's solution. Figure 8(b) also gives a sense of the accuracy of the approximate Mindlin and Levinson plate theories.

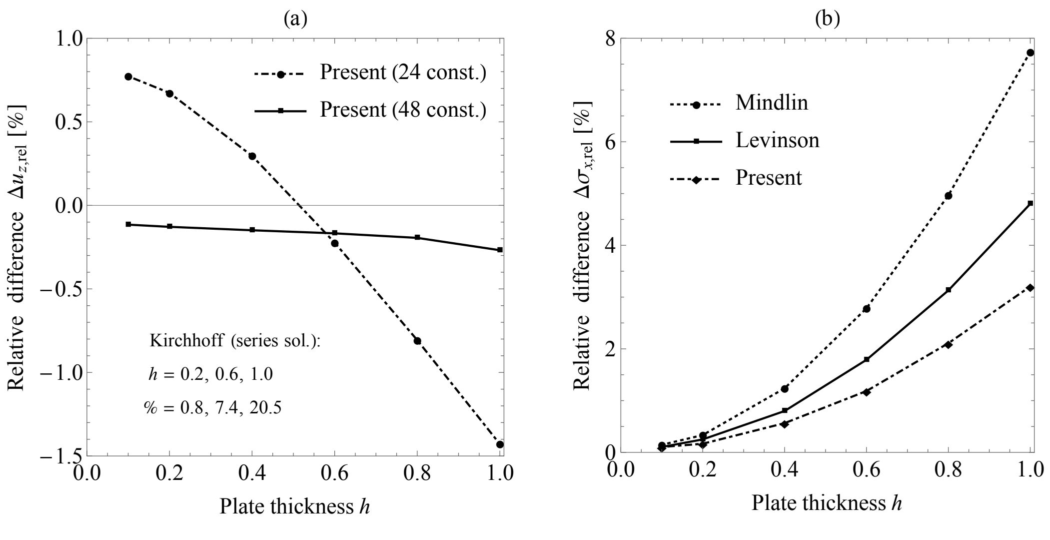

Figure 8: a) Relative difference between the present solution and Piltner's 3D solution (1988; 1992b) in terms of maximum transverse deflection. The relative difference between Kirchhoff and Piltner solutions is also given for three plate thicknesses. b) Relative difference for different plates in terms of $\sigma_x(0,0,-h/2)$ with Piltner's 3D solution as the reference.

5.4. All edges simply-supported – edge moments

As our final example, we consider a simply-supported rectangular plate subjected to uniformly distributed bending moments $M_0 = 1$ along edges $x = \pm a$ ($p_0 = 0$). For parameter values $a = 3$, $b = 2$, $E = 1$, $\nu = 0.3$, $h = 0.2$, we obtain at the center of the plate $M_x/M_0 = 0.0465$ and $M_y/M_0 = 0.2641$. Corresponding values obtained for a Kirchhoff plate by a series solution procedure are practically the same, i.e., $M_x/M_0 = 0.0465$ and $M_y/M_0 = 0.2635$ (Reddy, 2006). Figure 9 shows the displacement $u_z(x, y)$ for $a/b = 2$. Different types of concentrated line loads can be applied on the plate edges via the constraint conditions.

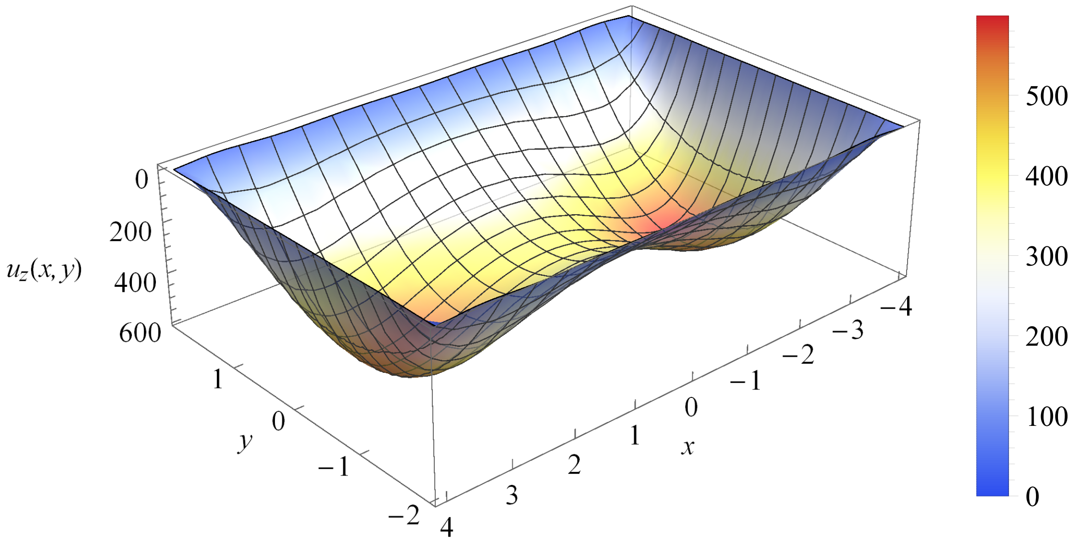

Figure 9: Simply-supported rectangular plate subjected to uniformly distributed bending moments along edges $x = \pm a$ ($p_0 = 0$).

6. Concluding remarks

In this paper, we presented a general 3D elasticity solution for a rectangular, isotropic, homogeneous plate in the conventional form of 2D plate theories. This was done by using 2D mid-surface variables formed from the 3D solution. The study was carried out in an interior framework without considering edge effects. The interior aspect allowed us to establish a clear connection between well-known 2D plate theories and 3D interior elasticity solutions. For one thing, the 2D interior plate equations developed from the 3D elasticity solution were shown to include the Kirchhoff, Mindlin and Levinson plate theories and their exact general solutions as special cases. We stress the salient feature of conventional 2D plates that they consist only of an interior part and, thus, do not have boundary layers. This amounts to interior stresses being active all-over of a conventional plate, including the lateral plate edges where the stresses act as surface tractions and contribute to the total potential energy of the plate. It is crucial to account for this property in all energy-based considerations. The literature is abundant with plate studies founded on interior kinematics that neglect the work contribution due to the interior stresses along the plate edges causing the studied plates to suffer from a number of unpleasant features such as interconnected artificial edge effects and governing differential equations of unnecessary complexity.

We considered only a rectangular interior plate. However, the general interior solution in Eqs. (6)–(8) may be transformed to other coordinate systems to investigate, for example, circular or elliptic interior plates. Furthermore, shell structures may be studied by taking into account the membrane part of the solution in all developments. The general solution may also be used to develop nodally-exact finite elements in the same way as in the case of elasticity-based interior beams (cf. Karttunen and von Hertzen, 2016a,c). The finite element approach also provides the exact shape functions for the interior structure at hand and the shape functions may be used, for example, as optimal first approximations in refined finite element formulations which include the nonlinear von Kármán strains. In addition, the presented theoretical plate considerations provide a starting point for the formulation of accurate isoparametric interior plate finite elements, and also facilitate the development of other numerical solution methods for interior plates such as isogeometric analysis (for reference, see the works of Kiendl et al. (2009) and Thai et al. (2014)). To sum it all up, formulation of structural problems within a clearly defined interior framework paves way for a multitude of refined analytical and numerical approaches for beams, plates and shells.

Appendix A. Mid-surface variables with uniform load $p = p_0$

$$\begin{Bmatrix} u_x(x,y) \\ u_y(x,y) \\ u_z(x,y) \\ \phi_x(x,y) \\ \phi_y(x,y) \end{Bmatrix} = \frac{1}{2G} \begin{Bmatrix} \left[(1+\nu) - \frac{h^2}{24}(3+4\nu)\nabla^2\right]\frac{\partial H}{\partial x} - 2\nabla^2\Phi_x + \frac{p_0\nu x}{2E} \\ \left[(1+\nu) - \frac{h^2}{24}(3+4\nu)\nabla^2\right]\frac{\partial H}{\partial y} - 2\nabla^2\Phi_y + \frac{p_0\nu y}{2E} \\ \Psi - \frac{p_0(1+\nu)}{16Eh^3}\left[3(\nu-1)(x^2+y^2)^2 + 6\nu h^2(x^2+y^2)\right] \\ -\frac{\partial}{\partial x}\left[\Psi + \frac{h^2}{4(1-\nu)}\nabla^2\Psi\right] + \frac{3p_0x(1+\nu)}{4Eh^3}\left[h^2(\nu-2) + (\nu-1)(x^2+y^2)\right] \\ -\frac{\partial}{\partial y}\left[\Psi + \frac{h^2}{4(1-\nu)}\nabla^2\Psi\right] + \frac{3p_0y(1+\nu)}{4Eh^3}\left[h^2(\nu-2) + (\nu-1)(x^2+y^2)\right] \end{Bmatrix}. \tag{A.1}$$

Eqs. (A.1) satisfy relations (11) and $(12)_1$ but not Eq. $(12)_2$, i.e.,

$$\frac{\partial \phi_x}{\partial x} + \frac{\partial \phi_y}{\partial y} + \nabla^2 u_z = -\frac{3p_0(1+\nu)}{Eh}\,. \tag{A.2}$$

Appendix B. Biharmonic polynomial $P(x, y)$

In Eq. (83), we have

$$P(x,y) = P_6 + P_7 + P_8 + P_9 + P_{10} + P_{11} + P_{12} + P_{13}, \tag{B.1}$$

where

$$
\begin{aligned}
P_6(x,y) &= c_{19}(3x^5y - 5x^3y^3) \\
&+ c_{20}(3xy^5 - 5x^3y^3) \\
&+ c_{21}(x^6 - 10x^4y^2 + 5x^2y^4) \\
&+ c_{22}(5x^4y^2 - 10x^2y^4 + y^6), \\
P_7(x,y) &= c_{23}(x^7 - 35x^3y^4 + 14xy^6) \\
&+ c_{24}(y^7 - 35y^3x^4 + 14yx^6) \\
&+ c_{25}(x^7 - 21x^5y^2 + 35x^3y^4 - 7xy^6) \\
&+ c_{26}(7x^6y - 35x^4y^3 + 21x^2y^5 - y^7), \\
P_8(x,y) &= c_{27}x(x^7 - 21x^5y^2 + 35x^3y^4 - 7xy^6) \\
&+ c_{28}y(x^7 - 21x^5y^2 + 35x^3y^4 - 7xy^6) \\
&+ c_{29}(x^8 - 28x^6y^2 + 70x^4y^4 - 28x^2y^6 + y^8) \\
&+ c_{30}(8x^7y - 56x^5y^3 + 56x^3y^5 - 8xy^7), \\
P_9(x,y) &= c_{31}x(x^8 - 28x^6y^2 + 70x^4y^4 - 28x^2y^6 + y^8) \\
&+ c_{32}y(x^8 - 28x^6y^2 + 70x^4y^4 - 28x^2y^6 + y^8) \\
&+ c_{33}(x^9 - 36x^7y^2 + 126x^5y^4 - 84x^3y^6 + 9xy^8) \\
&+ c_{34}(9x^8y - 84x^6y^3 + 126x^4y^5 - 36x^2y^7 + y^9), \\
P_{10}(x,y) &= c_{35}x(x^9 - 36x^7y^2 + 126x^5y^4 - 84x^3y^6 + 9xy^8) \\
&+ c_{36}y(x^9 - 36x^7y^2 + 126x^5y^4 - 84x^3y^6 + 9xy^8) \\
&+ c_{37}(x^{10} - 45x^8y^2 + 210x^6y^4 - 210x^4y^6 + 45x^2y^8 - y^{10}) \\
&+ c_{38}(10x^9y - 120x^7y^3 + 252x^5y^5 - 120x^3y^7 + 10xy^9), \\
P_{11}(x,y) &= c_{39}x(x^{10} - 45x^8y^2 + 210x^6y^4 - 210x^4y^6 + 45x^2y^8 - y^{10}) \\
&+ c_{40}y(x^{10} - 45x^8y^2 + 210x^6y^4 - 210x^4y^6 + 45x^2y^8 - y^{10}) \\
&+ c_{41}(11x^{10}y - 165x^8y^3 + 462x^6y^5 - 330x^4y^7 + 55x^2y^9 - y^{11}) \\
&+ c_{42}(x^{11} - 55x^9y^2 + 330x^7y^4 - 462x^5y^6 + 165x^3y^8 - 11xy^{10}), \\
P_{12}(x,y) &= c_{43}x(11x^{10}y - 165x^8y^3 + 462x^6y^5 - 330x^4y^7 + 55x^2y^9 - y^{11}) \\
&+ c_{44}y(11x^{10}y - 165x^8y^3 + 462x^6y^5 - 330x^4y^7 + 55x^2y^9 - y^{11}) \\
&+ c_{45}(x^{12} - 66x^{10}y^2 + 495x^8y^4 - 924x^6y^6 + 495x^4y^8 - 66x^2y^{10} + y^{12}) \\
&+ c_{46}(12x^{11}y - 220x^9y^3 + 792x^7y^5 - 792x^5y^7 + 220x^3y^9 - 12xy^{11}), \\
P_{13}(x,y) &= c_{47}(x^{13} - 78x^{11}y^2 + 715x^9y^4 - 1716x^7y^6 + 1287x^5y^8 - 286x^3y^{10} + 13xy^{12}) \\
&+ c_{48}(13x^{12}y - 286x^{10}y^3 + 1287x^8y^5 - 1716x^6y^7 + 715x^4y^9 - 78x^2y^{11} + y^{13}).
\end{aligned}
\tag{B.2}
$$

Acknowledgements

The financial support from the Ministry of Education and Culture of Finland through the Graduate School of Engineering Mechanics is gratefully acknowledged by the first author. In addition, the authors acknowledge the Finland Distinguished Professor (FiDiPro) programme: "Non-linear response of large, complex thin-walled structures" supported by Tekes (The Finnish Funding Agency for Technology and Innovation) and industrial partners Napa, SSAB, Deltamarin, Koneteknologiakeskus Turku and Meyer Turku.

References

Barber, J. R., 2010. Elasticity, 3rd Edition. Springer, New York.

Barrett, K. E., Ellis, S., 1988. An exact theory of elastic plates. Int. J. Solids Struct. 24 (9), 859–880.

Batista, M., 2012. Comparison of Reissner, Mindlin and Reddy plate models with exact three dimensional solution for simply supported isotropic and transverse inextensible rectangular plate. Meccanica 47 (1), 257–268.

Batista, M., 2015. An exact theory of the bending of transversely inextensible elastic plates. Acta Mech. 226 (9), 2899–2924.

Bert, C. W., 1984. A critical evaluation of new plate theories applied to laminated composites. Compos. Struct. 2 (4), 329–347.

Cheng, S., 1979. Elasticity theory of plates and a refined theory. J. App. Mech. 46 (3), 644–650.

Cooke, D. W., Levinson, M., 1983. Thick rectangular plates-II: The generalized Lévy solution. Int. J. Mech. Sci. 25 (3), 207–215.

Demasi, L., 2007. Three-dimensional closed form solutions and exact thin plate theories for isotropic plates. Compos. Struct. 80 (2), 183–195.

Gregory, R. D., 1992. The general form of the three-dimensional elastic field inside an isotropic plate with free faces. J. Elast. 28 (1), 1–28.

Gregory, R. D., Wan, F. Y. M., 1985. On plate theories and Saint-Venant's principle. Int. J. Solids Struct. 21 (10), 1005–1024.

Jemielita, G., 1990. On kinematical assumptions of refined theories of plates – a survey. J. Appl. Mech. 57 (4), 1088–1091.

Karttunen, A. T., von Hertzen, R., 2015. Variational formulation of the static Levinson beam theory. Mech. Res. Commun. 66, 15–19.

Karttunen, A. T., von Hertzen, R., 2016a. Exact theory for a linearly elastic interior beam. Int. J. Solids Struct. 78, 125–130.

Karttunen, A. T., von Hertzen, R., 2016b. Interior formulation of axisymmetric Levinson plate theory. Mech. Res. Commun. Under review.

Karttunen, A. T., von Hertzen, R., 2016c. On the foundations of anisotropic interior beam theories. Compos. B-Eng. 87, 299–310.

Kiendl, J., Bletzinger, K.-U., Linhard, J., Wüchner, R., 2009. Isogeometric shell analysis with Kirchhoff–Love elements. Comput. Method. Appl. M. 198 (49), 3902–3914.

Levinson, M., 1980. An accurate, simple theory of the statics and dynamics of elastic plates. Mech. Res. Commun. 7 (6), 343–350.

Levinson, M., 1985. The simply supported rectangular plate: An exact, three dimensional, linear elasticity solution. J. Elast. 15 (3), 283–291.

Levinson, M., Cooke, D. W., 1983. Thick rectangular plates-I: The generalized Navier solution. Int. J. Mech. Sci. 25 (3), 199–205.

Mindlin, R. D., 1951. Influence of rotary inertia and shear on flexural motions of isotropic, elastic plates. J. App. Mech. 18, 31–38.

Nguyen, T., Thai, C. H., Nguyen-Xuan, H., 2016. On the general framework of high order shear deformation theories for laminated composite plate structures: A novel unified approach. Int. J. Mech. Sci. 110, 242–255.

Nosier, A., Reddy, J. N., 1992. On boundary layer and interior equations for higher-order theories of plates. ZAMM-Z. Angew. Math. Me. 72 (12), 657–666.

Piltner, R., 1988. The application of a complex 3-dimensional elasticity solution representation for the analysis of a thick rectangular plate. Acta Mech. 75 (1-4), 77–91.

Piltner, R., 1991. Three-dimensional stress and displacement representations for plate problems. Mech. Res. Commun. 18 (1), 41–49.

Piltner, R., 1992a. The derivation of a thick and thin plate formulation without ad hoc assumptions. J. Elast. 29 (2), 133–173.

Piltner, R., 1992b. A quadrilateral hybrid-Trefftz plate bending element for the inclusion of warping based on a three-dimensional plate formulation. Int. J. Numer. Met. Eng. 33 (2), 387–408.

Reddy, J. N., 1984. A simple higher–order theory for laminated composite plates. J. Appl. Mech. 51 (4), 745–752.

Reddy, J. N., 1990. A general nonlinear 3rd–order theory of plates with moderate thickness. Int. J. Nonlin. Mech. 25 (6), 677–686.

Reddy, J. N., 2003. Mechanics of Laminated Composite Plates and Shells: Theory and Analysis, 2nd Edition. CRC Press, Boca Raton, Florida.

Reddy, J. N., 2006. Theory and analysis of elastic plates and shells. CRC press.

Reddy, J. N., Kim, J., 2012. A nonlinear modified couple stress-based third-order theory of functionally graded plates. Compos. Struct. 94 (3), 1128–1143.

Reddy, J. N., Wang, C. M., Lim, G. T., Ng, K. H., 2001. Bending solutions of Levinson beams and plates in terms of the classical theories. Int. J. Solids Struct. 38 (26), 4701–4720.

Sadd, M. H., 2014. Elasticity – Theory, Applications and Numerics, 3rd Edition. Academic Press, Oxford.

Savoia, M., Reddy, J. N., 1992. A variational approach to three-dimensional elasticity solutions of laminated composite plates. J. Appl. Mech. 59 (2S), S166–S175.

Srinivas, S., Rao, A. K., 1970. Bending, vibration and buckling of simply supported thick orthotropic rectangular plates and laminates. Int. J. Solids Struct. 6 (11), 1463–1481.

Srinivas, S., Rao, A. K., 1973. Flexure of thick rectangular plates. J. App. Mech. 40 (1), 298–299.

Srinivas, S., Rao, A. K., Joga Rao, C. V., 1969. Flexure of simply supported thick homogeneous and laminated rectangular plates. ZAMM-Z. Angew. Math. Me. 49 (8), 449–458.

Szilard, R., 2004. Theories and applications of plate analysis: classical numerical and engineering methods. John Wiley & Sons.

Thai, C. H., Kulasegaram, S., Tran, L. V., Nguyen-Xuan, H., 2014. Generalized shear deformation theory for functionally graded isotropic and sandwich plates based on isogeometric approach. Comput. Struct. 141, 94–112.

Timoshenko, S. P., Goodier, J. N., 1970. Theory of Elasticity, 3rd Edition. McGraw-Hill, Singapore.

Timoshenko, S. P., Woinowsky-Krieger, S., 1959. Theory of Plates and Shells, 2nd Edition. McGraw-Hill, New York.

Vinson, J. R., 2006. Plate and panel structures of isotropic, composite and piezoelectric materials, including sandwich construction. Springer, New York.

Vlasov, B. F., 1957. On equations of bending of plates (in Russian). Dokla Ak. Nauk Azerbeijanskoi SSR 3, 955–959.

Wang, F. Y., 1990. Two-dimensional theories deduced from three-dimensional theory for a transversely isotropic body. I: Plate problems. Int. J. Solids Struct. 26 (4), 455–470.

Wang, F. Y., 1991. Two-dimensional theories deduced from three-dimensional theory for a transversely isotropic body. II: Plane problems. Int. J. Solids Struct. 28 (2), 161–177.

Wang, M. Z., Zhao, B. S., 2003. The decomposed form of the three-dimensional elastic plate. Acta Mech. 166 (1-4), 207–216.

Zhao, B., Wu, D., Wang, M., 2013. The refined theory and the decomposed theorem of a transversely isotropic elastic plate. Eur. J. Mech. A-Solid. 39, 243–250.